Nuclear Materials and Energy 42 (2025) 101893

Contents lists available at ScienceDirect

Nuclear Materials and Energy

journal homepage: www.elsevier.com/locate/nme

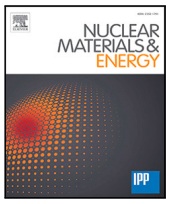

Characterization of detachment inferred from the Balmer line ratios in JET-ILW low-confinement mode plasmas

Vesa-Pekka Rikala [a,*], M. Groth [a], A.G. Meigs [b], D. Reiter [c], B. Lomanowski [b,d], A. Shaw [b], S. Aleiferis [b], G. Corrigan [b], I.S. Carvalho [b,e], D. Harting [b,f], N. Horsten [a,g], I. Jepu [b], J. Karhunen [a,h,b], K.D. Lawson [b], C. Lowry [b], S. Menmuir [b], B. Thomas [b], D. Borodin [f], D. Douai [i], A. Huber [b,f], JET Contributors [1]

[a] Aalto University, Department of Applied Physics, Espoo, Finland
[b] UKAEA, Culham Science Centre, Abingdon, UK
[c] Heinrich Heine University Düsseldorf, Düsseldorf, Germany
[d] Oak Ridge National Laboratory, USA
[e] ITER Organization, Route de Vinon-sur-Verdon, CS 90 046, 13067 St. Paul Lez Durance Cedex, France
[f] Forschungszentrum Jülich GmbH, Institut für Energie- und Klimaforschung - Plasmaphysik, Partner of the Trilateral Euregio Cluster (TEC), Jülich, Germany
[g] KU Leuven, Leuven, Belgium
[h] University of Helsinki, Helsinki, Finland
[i] CEA IFRM Cadarache, France

ARTICLE INFO

Keywords:
Fusion
Scrape-off layer
Divertor visible spectroscopy
EDGE2D
EIRENE

ABSTRACT

Spectroscopic measurements of the hydrogenic Balmer-α and Balmer-γ line emission in JET-ILW low-confinement mode (L-mode) deuterium plasmas are used to assess the onset of volume recombination in the low-field side (LFS) divertor. The evolution of the EDGE2D-EIRENE predicted Balmer-γ to Balmer-α emission ratio from low-recycling to detached conditions is in qualitative agreement with the measured ratio. In low-recycling conditions the EDGE2D-EIRENE predicted line-emission is within 30% of measured emission, in high-recycling within 20%t, and in detached conditions lower by a factor of 2.5.

1. Introduction

Detached divertor conditions are the preferred plasma conditions in fusion devices, due to the low electron temperature at the target and the high radiated power fraction, thus, reduced particle heat fluxes to the divertor target plates [1]. High particle and heat fluxes to the targets erode material from the targets, thus, increase the impurity contents of the plasma, which negatively impacts the fusion power gain. Additionally, the shielding of an ITER-like wall (ILW) divertor tiles is important for the survival of the target tiles, such that the tiles do not evaporate, or melt and recrystallize. Previous studies in JET-C (Carbon) used Balmer-γ to Balmer-α line ratio to infer the presence of volume recombination, thus, detached divertor conditions [2]. Ratios of Lyman lines have been used in DIII-D to distinguish ionizing and recombining plasma conditions in the divertor [3]. The Balmer- and Lyman-line emission are the emission from the de-excitation of the hydrogenic atom from the principal quantum number p to the state 2 and 1, respectively. Additionally, in the JET-ILW, 2D tomographic reconstructions from a toroidally viewing endoscope system has been used to measure the Balmer-α and Balmer-γ line emission in high-confinement mode (H-mode) [4], and in L-mode, in which the reconstruction was improved by taking into account reflected light from the metallic wall in JET-ILW [5].

The primary objective of this study is to characterize detachment of the low-field side (LFS) divertor in JET-ILW low-confinement mode (L-mode) plasmas using Balmer-γ/Balmer-α line ratios, and to validate these findings against EDGE2D-EIRENE simulations. EDGE2D is a 2D multi-fluid code iteratively coupled with the 3D neutral Monte Carlo code EIRENE [6,7], developed by JET under the JET Joint Undertaking, in parallel to SOLPS-ITER [8]. SOLPS-ITER is an alternative 2D multi-fluid code to EDGE2D-EIRENE, and both codes solve a similar set of 2D fluid equations. EIRENE is the common neutral Monte Carlo code in both EDGE2D-EIRENE and SOLPS-ITER, thus, any differences

* Corresponding author.
E-mail address: vesa-pekka.rikala@aalto.fi (V.-P. Rikala).

[1] "See the author list of "Overview of T and D-T results in JET with ITER-like wall" by CF Maggi et al., Nuclear Fusion (2024), DOI 10.1088/1741-4326/ad3e16".

https://doi.org/10.1016/j.nme.2025.101893
Received 17 May 2024; Received in revised form 9 January 2025; Accepted 1 February 2025
Available online 10 February 2025

between the codes are due to differences in the predicted background plasmas. The focus is on the L-mode plasmas due to better availability of systematic measurements over range of core plasma densities, and due to the simpler plasma conditions in L-mode, since L-mode avoids divertor plasma perturbations due to Edge Localized modes (ELMs). Additionally, L-mode plasma have lower radial and poloidal gradiens, thus, permitting cross-field drifts in EDGE2D-EIRENE, with no need for executing ELM models. The general strategy is to validate edge physics in the simpler L-mode plasmas first, and then move to H-mode with separate ELM-specific models.

The JET-ILW is a challenging environment for spectroscopy, compared to carbon based machines such as DIII-D or JET-C, due to the highly reflective metallic wall in JET-ILW, which amplifies the observed emission. To accurately compare simulations to experiment, the ray-tracing code Cherab is used to account for reflections in the EDGE2D-EIRENE predicted plasmas [9]. Cherab has previously been used in assessing both the experimentally observed emission, and the EDGE2D-EIRENE predicted emission [5]. It was found that in experiment, the brightest regions were amplified by 15% to 20 % in the tomographic reconstruction due to reflections. When the tomographic image was used to produce synthetic spectroscopy by integrating the emission along lines-of-sight, the emission was amplified by 15% to 25% at the target strike-points, which agreed with the synthetic spectroscopy on the EDGE2D-EIRENE predicted plasma background.

It is expected that volumetric recombination [2], a process in which the plasma ions recombine with the electrons to form neutral particles in the plasma, become the dominant sources of emission in regions with low electron temperature $T_e < 2$ eV, when the divertor conditions evolve from high-recycling to partially detached, while in high-recycling conditions the molecularly induced emission is expected to dominate [10,11]. High-recycling conditions are characterized by significant temperature gradients in the SOL, and quadratic scaling of the target flux to upstream plasma density. In partially detached conditions the temperature of the plasma at the target is low enough for a neutral gas front to form between the divertor target and the plasma. Since recombination populates the high principal quantum number excitation levels more, relative to electron impact excitation [12], it is expected that Balmer-γ emission increases more relative to Balmer-α, with increasing degree of detachment.

2. Experiment and EDGE2D-EIRENE simulation setup

Low-confinement mode (L-mode) plasmas with the toroidal magnetic field set to $B_t = 2.5$ T, the plasma current to $I_p = 2.45$ MA, and 1 MW of neutral beam injection (NBI) heating, are analysed in these studies. Ohmic heating ranges from 1.6 MW to 2.2 MW, thus, the total heating power is in the range of 2.6 MW to 3.2 MW. Experimentally, interferometer measurements [13] of the electron density at the plasma edge are used as representative measurements of the plasma conditions at the LFS midplane. (Fig. 1) [14]. The JET pulses analysed in this work consist of density step pulses (JPN 96767, 96770, 96771, 96772), in which the plasma density is raised in steps and held constant for short intervals, and of density ramp pulses (JPN 96759–96762), in which the plasma density is continuously increased.

The low-field side (LFS) divertor in JET-ILW has comprehensive coverage of multiple spectroscopy instruments (Fig. 1), which are used to measure the deuterium Balmer-α line emission. These instruments include a vertical poloidally scanning spectrometer (KT1V) [15], a filterscope spectroscopy system (KS3O) [16], and a mirror-linked filtered imaging spectrometer subsystem (kt3e8ta), which utilizes the lost light from the mirror-link [17,18]. The deuterium Balmer-γ line is also measured using the lost-light system (kt3e8tb) [18]. Additionally, a toroidally viewing endoscope system (KL11) is used for measuring Balmer-α and Balmer-γ emission [19], by reconstructing a 2D poloidal view, and line integrating along the KT3 lines-of-sight (LOS), to produce comparable data. For low- and high-recycling conditions

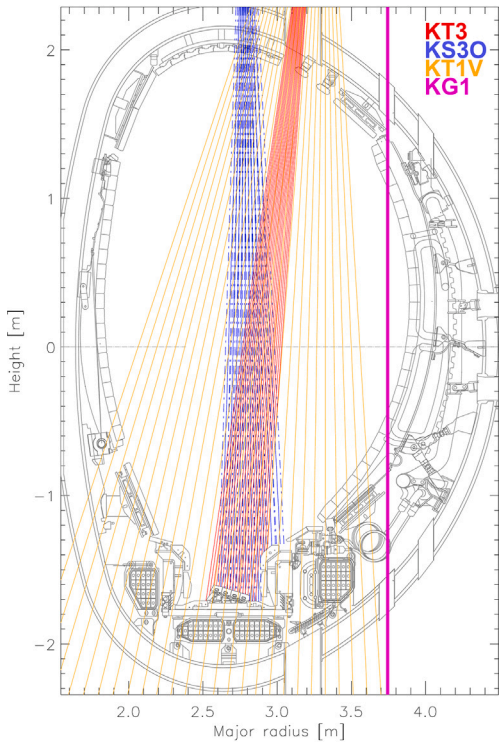

Fig. 1. Lines-of-sight of the spectroscopic systems, which are the kt3e8ta/b filtered imaging systems utilizing the lost light from the KT3 spectrometer (red) [18], the low-field side filterscope spectroscopy system KS30 (blue) [16], the vertical poloidally scanning spectrometer KT1V (orange) [15], and the edge interferometer KG1 (magenta) [13]. (For interpretation of the references to colour in this figure legend, the reader is referred to the web version of this article.)

Langmuir probes (LP) on the LFS divertor are used to measure the electron temperature and density, T_e and n_e, respectively, and using the ADAS inverse photon efficiency coefficients [20], estimates for Balmer-α and Balmer-γ emission are derived. The measurement error is two standard deviations of the time-averaged measurement data.

In the measurements, the KT1V mirror-link system had a sweep cycle time of 130 ms, the filterscope system KS3O has a sampling rate of 10 kHz, the kt3e8ta a sampling rate of 1 kHz, and the kt3e8tb a sampling rate of 200 Hz. In the comparison to simulations, the measurements are averaged over 1.0 s at a constant plasma density, except for low-recycling conditions, in which the measurement are averaged over 0.1 s, due to the only available low-recycling data being from a density ramp pulse. The KT1V sweep cycle time is a significant limitation in the low-recycling conditions, due to the short available time for time averaging. Additionally, there is uncertainty in the position of the line-of-sight of the KT1V system on the divertor, caused by uncertainty in the position of the mirror. The Langmuir probe data is averaged over 0.05 s in low-recycling conditions, and over 2.0 s in high-recycling conditions.

The 2D multi-fluid code EDGE2D [6], iteratively coupled with the 3D neutral Monte Carlo code EIRENE [7], is used to produce 2D maps of the plasma and neutral parameters in the plasma edge. Anomalous radial transport of plasma species is set *ad-hoc*, using particle diffusion ($D_\perp$) and heat conduction ($\chi_{\alpha,\perp}$) coefficients. The LFS midplane electron density at the separatrix $n_{e,sep,LFS-mp}$ is used as the control parameter in the simulations. In this work the plasma species are electrons, deuterium ions, and beryllium ions as the impurity species. The neutral species are deuterium and beryllium atoms and deuterium molecules. Molecular ions D_2^+ are included in the EIRENE simulation, but are assumed to react immediately at the point of creation, i.e., a static approximation. The data sources for the atomic and molecular

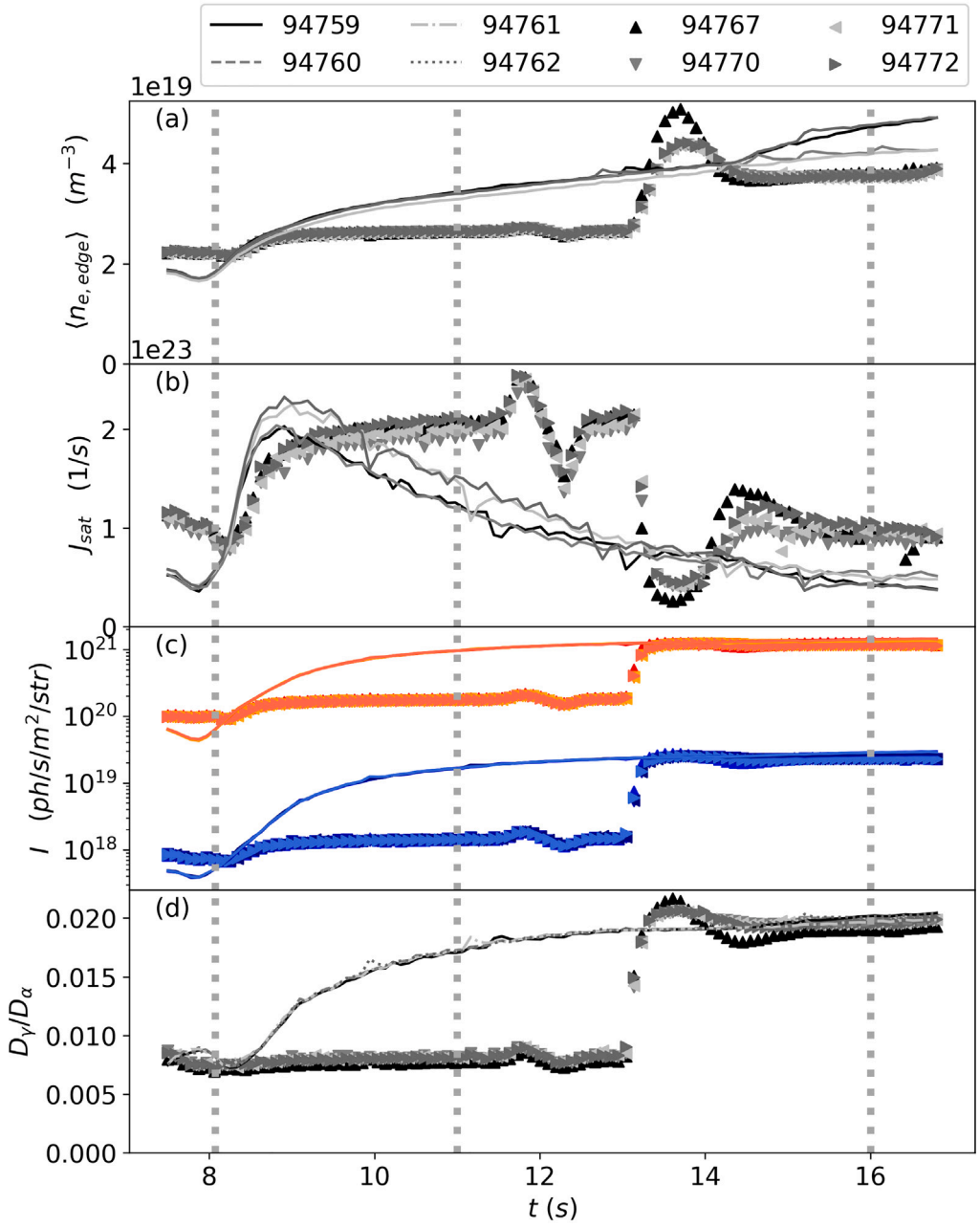

Fig. 2. The edge electron density measured by KG1 (a), the LFS divertor ion saturation current (b), the KT3e8Ta/b measured Balmer-α and Balmer-γ line emission (c), and the ratio of Balmer-α to Balmer-α (d), averaged over the JET divertor tile-5 area, as a function of time. The solid lines are the density ramp pulses, and markers are the density step pulses. The dashed vertical lines mark the low-recycling (8.1 s), high-recycling (11 s), and detached conditions (16 s), which are compared against EDGE2D-EIRENE simulations.

deuterium species are the HYDHEL and AMJUEL databases [12,21], and ADAS for the beryllium processes [20]. The atomic and molecular reactions in HYDHEL and AMJUEL are composed of polynomial fits, thus, have an associated fitting error. Additionally, it is assumed that the rates for hydrogen are identical to those for deuterium, and that it is sufficient to scale the collision energies associated with the rates by the mass ratio of deuterium to hydrogen. The ADAS database is composed of tabulated data as a function of temperature and density. The reaction cross-sections are extracted by interpolating the data, thus, introducing interpolation error. The estimation of the error of the atomic and molecular sources is out of the scope of this paper, since the plasma is coupled to the neutrals, and will change as the plasma-neutral interaction rates are changed.

The input power crossing the EDGE2D-EIRENE core boundary is set to 2.2 MW, divided evenly between electrons and fuel ions, for all values of $n_{e,sep,LFS-mp}$. It is assumed that the core radiated power increases such that the increase in Ohmic heating is negated, thus, maintaining a constant heating power. The anomalous diffusion coefficient $D_\perp$ is set to vary, such that in the core plasma $D_\perp = 1.0$ m^2/s, at -1.0 cm $< R - R_{sep} < 1.0$ cm $D_\perp = 0.5$ m^2/s, and at $R - R_{sep} > 1.0$ cm in the SOL $D_\perp = 1.0$ m^2/s. The $\chi_{\alpha,\perp}$ is set to equal for all the plasma species, and vary, such that, in the core to the separatrix $\chi_{\alpha,\perp} = 1.0$ m^2/s, and in the SOL $\chi_{\alpha,\perp} = 0.5$ m^2/s. The parameter values for $D_\perp$ and $\chi_{\alpha,\perp}$ were derived in Ref. [14], in which the values were determined by matching the EDGE2D-EIRENE predicted T_e and n_e profiles at the LFS midplane to measurements from high-resolution Thomson scattering (T_e, n_e), and to lithium beam injection (n_e) in low-recycling conditions (see Fig. 9

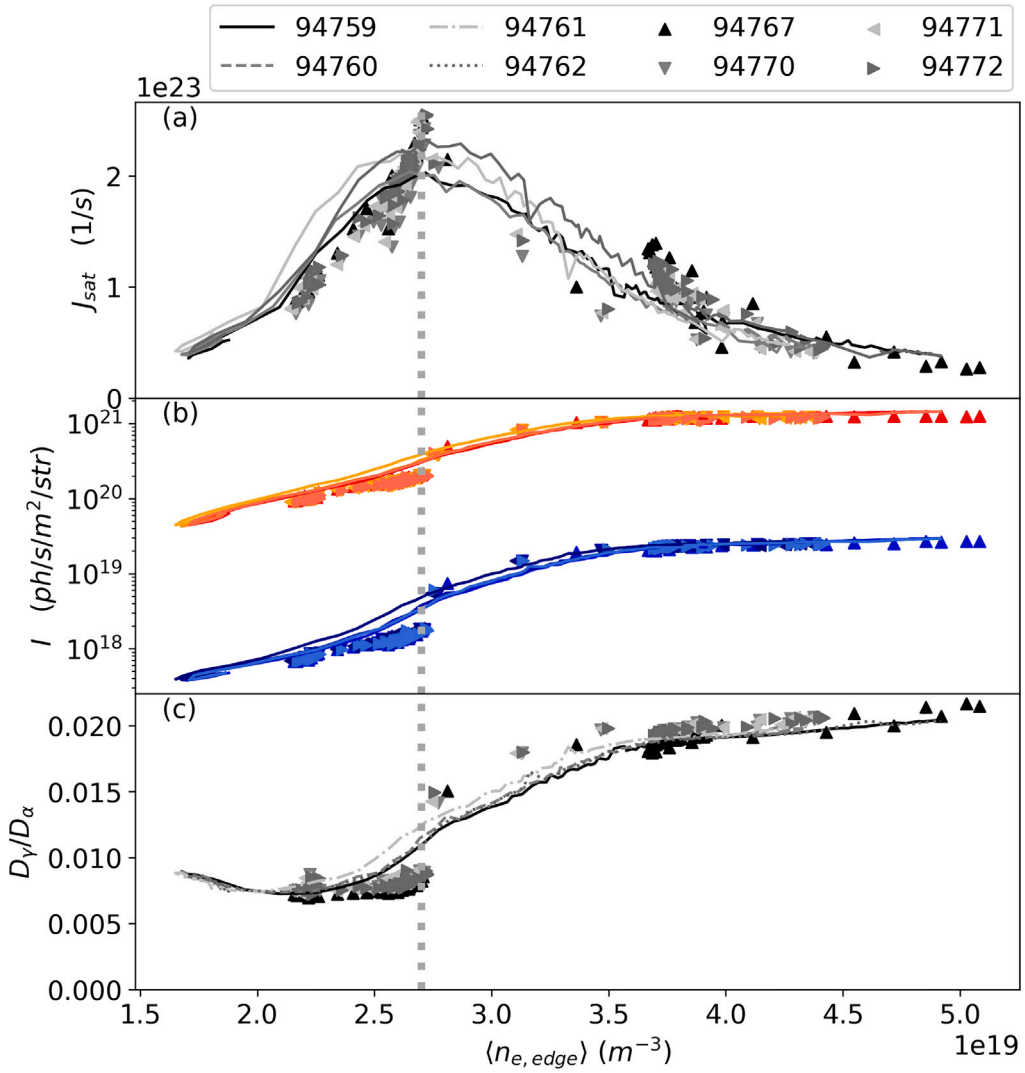

Fig. 3. The LFS divertor ion saturation current (a), the KT3e8Ta/b measured Balmer-α and Balmer-γ line emission (b), and the ratio of Balmer-γ to Balmer-α (c), averaged over the JET divertor tile-5 area, as a function of edge line-averaged electron density. The solid lines are the density ramp pulses, and markers are the density step pulses. The dashed vertical line marks roll-over of the ion saturation current.

in [14]). In this work, drifts due to $\vec{E}\times\vec{B}$ and $\vec{B}\times\nabla B$, and thermo-electric currents are included.

The metallic wall in JET-ILW is highly reflective, which needs to be accounted for in the post-processing of the EDGE2D-EIRENE simulations. The ray-tracing code Cherab is used to calculate the total line emission, i.e. the direct emission from the excited neutral atomic population, which is calculated from the AMJUEL data [12] (See Appendix B), and the reflected light from the vessel walls [9,22]. In this work, measurements of the kt3e8ta/b systems are simulated using Cherab on EDGE2D-EIRENE predictions of the plasma and neutral conditions. The full JET-ILW CAD mesh is used, and for the metallic surface elements the surface roughness is 0.26 for beryllium elements, and 0.29 for tungsten elements. The Cherab model uses a fibre-optic observer, with no spectral binning. The molecular ion density $n_{D_2^+}$ is calculated using the AMJUEL rate for hydrogen, which is not fully valid in regions of plasma with low deuterium ion temperature, since the charge-exchange process $H_2+H^+ \rightarrow H_2^+ + H$ depends on the isotope mass, and is different for deuterium. Additionally, the rates are approximated at a constant H_2 temperature $T_{H_2} = 0.1$ eV.

3. Measurements and predictions of the Balmer line emission

The measurements are compared to EDGE2D-EIRENE predictions in three different plasma conditions, in low-recycling (8.1 s), in high-recycling (11 s), and in detached conditions (16 s) (Fig. 2). For the comparison, the pulse 94759 is chosen for the measurements in low-recycling conditions, and the pulse 94767 for the measurements in high-recycling and detached conditions. The EDGE2D-EIRENE controlling edge electron density is set to half of the KG1 measured edge density (Fig. 2a).

The kt3e8ta measured average intensity of the Balmer-α and Balmer-γ line emission across the JET-ILW LFS divertor increases exponentially with $\langle n_{e,edge}\rangle$ up to $\langle n_e\rangle \approx 3.8\cdot 10^{19}$ m^{-3}, and stagnates with higher electron density (Fig. 4b). Here, the radial profile of the line emission was integrated across the LFS (tile-5) target plate. In the density step pulses the profile of the ion saturation current J_{sat} is more peaked compared to the density ramp pulses. In the Balmer-α and Balmer-γ profiles of the step pulses, there is a sharp increase in intensity at the peak of J_{sat}, whereas in the density ramp pulses the transition over the peak of J_{sat} is smooth. The ratio of Balmer-γ to Balmer-α

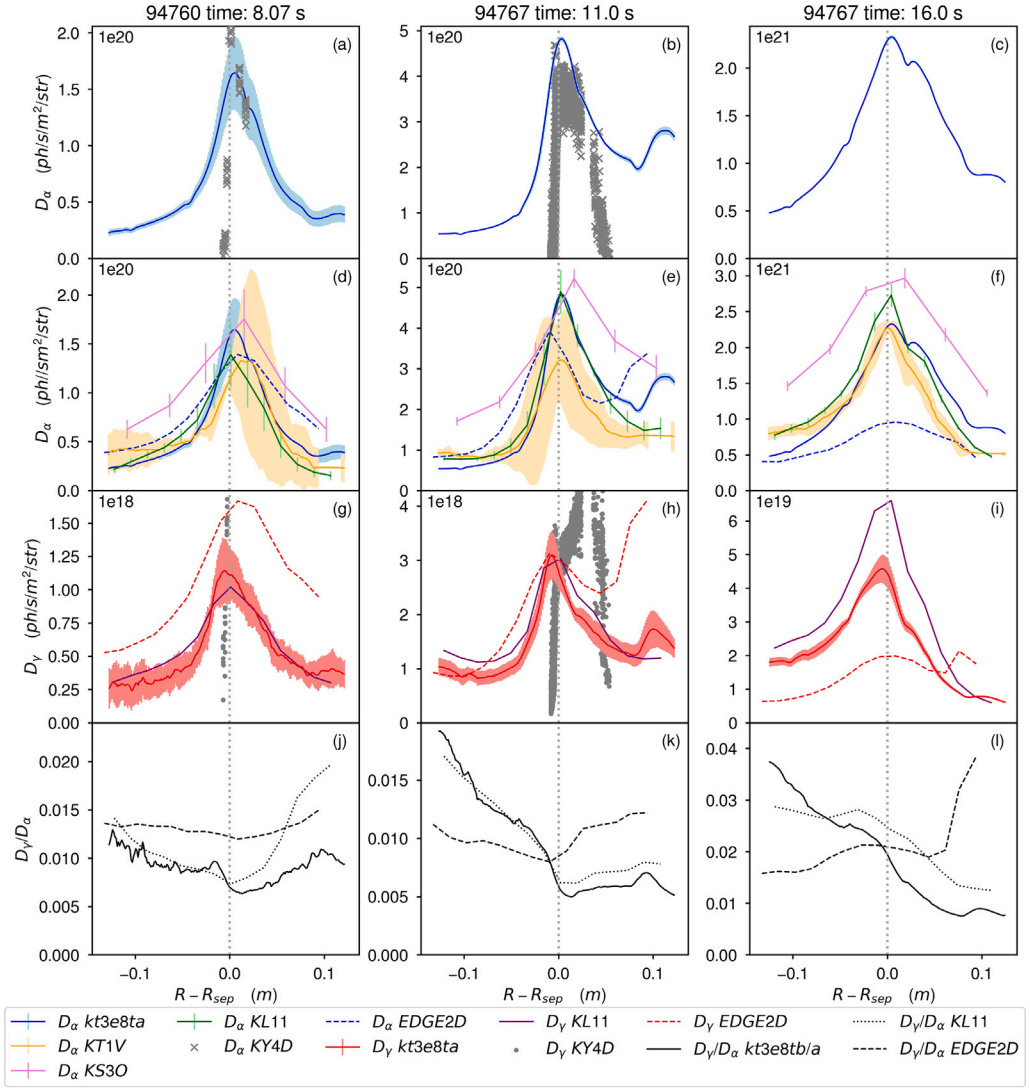

Fig. 4. Balmer-α (a, b, c, d, e, f) line emission measured by kt3e8ta (blue, solid), KT1V (orange), KS3O (purple), and KL11 (green) systems, and Balmer-γ (g, h, i) line emission measured by kte3e8tb (red, solid), and KL11 (dark purple), on the LFS divertor. The EDGE2D-EIRENE predicted Balmer-α (blue, dashed) and Balmer-γ (red, dashed) line emission use the kt3e8ta/b lines-of-sight. The ratio of Balmer-γ to Balmer-α (j, k, l) is calculated from the kt3e8ta and kte3e8tb (black, solid) and KL11 (black, dotted) measurements, and from the respective EDGE2D-EIRENE predictions (black, dashed). ADAS derived inverse photon efficiency coefficients are used to calculate Balmer-α (grey, x) and Balmer-γ (grey, dot) emissivity from LP measurements of T_e and n_e (JPN 94759, part of a series of repeat pulses, is used for a and d). The KT1V measurements are shifted to match the peak of the kt3e8ta measurement. The KL11 measurements are from JPN 94771, which is a repeat pulse of JPN 94767. Note that the error bars for Balmer-γ measured by KL11 are not shown, as the error is twice the range of the chart. (For interpretation of the references to colour in this figure legend, the reader is referred to the web version of this article.)

calculated from the kt3e8ta measurements reaches the value of 0.020 in detached conditions (Fig. 3c), consistent with previous measurements in JET with the carbon wall (JET-C), in which the ratio of the emission at the LFS divertor was measured to be approximately 0.02 in partially detached conditions [2]. At the edge density of the J_{sat} peak, the ratio of Balmer-γ to Balmer-α reaches a minimum value of 0.006. In the JET-ILW a ratios of 0.05 to 0.10 in partially detached H-mode conditions was reconstructed using an endoscope system [4], consistent with the ratio in this work, when accounting for the different operational modes.

The peak of the EDGE2D-EIRENE predicted Balmer-α emission in low-recycling conditions is within the measurement uncertainties of the kt3e8ta, KT1V, and KL11 measurements, and within 30% of the KS30 measurement (Fig. 4d). The KT1V measurement has large scatter due to combination of the oscillating mirror setup, and the plasma conditions changing in the density ramp pulse. The LP (KY4D) derived Balmer-α and Balmer-γ emission is within the same order of magnitude as the other measurements, as is expected in low-recycling conditions (Figs. 4a, g), in which the target T_e and n_e are peaked at the strike-point. The LP estimate for Balmer-α is also reliable for high-recycling conditions, but for Balmer-γ the LP derived profile peaks in the far-SOL (the edge of the SOL the furthest away from the separatrix) (Figs. 4b, h), contrary to spectroscopic measurements, which peak at the strike-point. The EDGE2D-EIRENE predicted Balmer-γ emission is higher by 30% compared to kt3e8tb and KL11 measurements in low-recycling conditions (Fig. 4g).

In high-recycling conditions the EDGE2D-EIRENE prediction replicates the double-peaked Balmer-α emission structure, as observed by the kt3e8ta instrument (Fig. 4e). For Balmer-γ a similar structure is observed, but the predicted emission is higher by a factor of 2 to 3.5 in the far-SOL (Fig. 4h). At low electron temperatures $T_e < 2$ eV the recombination rate increases exponentially with decreasing T_e, and with increasing n_e the rate also increases exponentially [12]. Therefore, EDGE2D-EIRENE overpredicts n_e, and underpredicts T_e in the far-SOL. The region of the Balmer-γ far-SOL peak corresponds to the LFS divertor tile 5 and tile 6 junction, in which the divertor surface drops by 5 cm (see Fig. 1). In simulations on a simplified grid, in which the tile transition is removed by raising the tile-6, with otherwise identical settings and control n_e, the predicted emission is lower by a factor of

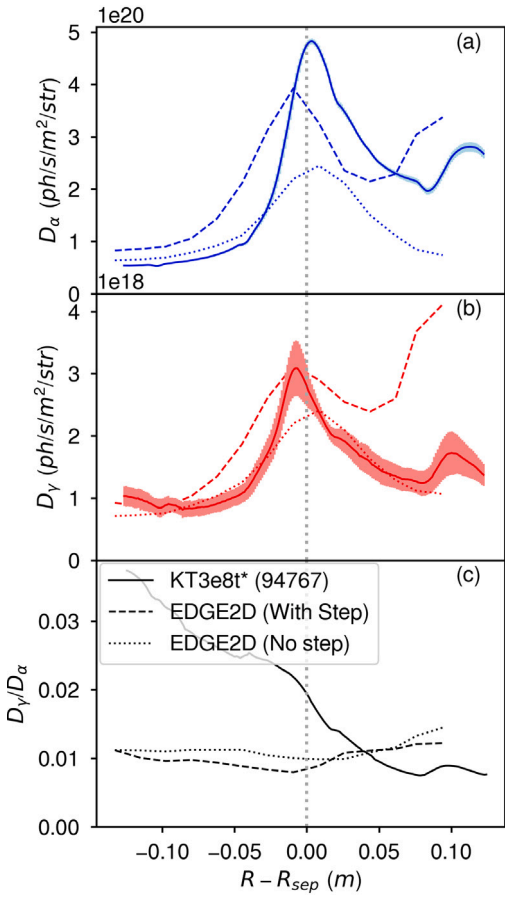

Fig. 5. EDGE2D-EIRENE predicted (with tile-5 to tile 6 step, dashed, no step, dotted) and KT3e8ta/b measured (solid) Balmer-α (a) and Balmer-γ (b) emission, and the ratio Balmer-γ to Balmer-α (c), on the LFS divertor. The dashed vertical line marks the location of the strike-point.

two (Figs. 5a–c). Additionally, a D_2^+ front (a high concentration of D_2^+ ions) is not formed, i.e. the plasma is in low-recycling conditions in the simplified grid with the same control density.

In all recycling conditions, the EDGE2D-EIRENE predicted profiles have longer fall-off lengths compared to measurements, which suggests that the n_e profile is wider in the simulations than in the experiment. Additionally, the inclusion of reflections increase the simulated emission by 30 to 50% in all recycling conditions. If the predicted n_e profile was more peaked, there would be fewer particles in the far-SOL, thus, fewer neutrals and D_2^+, and less emission. The simulations are, however, insensitive to changes in D_{perp}, as reduction by a factor of 10 does not lead to a significant peaking of the J_{sat} profiles.

For the plasmas with the highest $\langle n_{e,edge} \rangle$, the kt3e8ta, KT1V, and KL11 measured Balmer-α emission intensity is higher by a factor of 2.5, compared to the EDGE2D-EIRENE prediction (Fig. 4f). Compared to KS3O measured Balmer-α, the EDGE2D-EIRENE prediction is lower by a factor of 3. The Balmer-γ emission measured by kt3e8tb is, similarly to the measurements of Balmer-α, higher by a factor of 2.5 to 3, and for KL11 measurements higher by a factor of 3.5, compared to the EDGE2D-EIRENE prediction (Fig. 4i).

Quantitatively, EDGE2D-EIRENE fails to predict the profiles of the Balmer-γ to Balmer-α line emission ratios (Figs. 4j, k, l). The trend in the evolution of the averaged Balmer-γ/Balmer-α ratio over the LFS divertor as a function of edge electron density, i.e. evolution from Fig. 4j through Fig. 4k to Fig. 4l, qualitatively matches with experiment, as the ratio reaches its minimum in high-recycling (Fig. 4k) conditions, and increases to a maximum in detached conditions (Fig. 4l).

In low-recycling conditions, and in high-recycling up to the roll-over point of J_{sat} at $n_{e,sep,LFS-mp} = 1.4 \cdot 10^{19}$ m^{-3}, the Balmer-α emission is dominated by electron impact excitation in the EDGE2D-EIRENE simulations (Figs. 6a, b, c), as is expected in ionizing plasma conditions. Past the roll-over of J_{sat}, the dissociative recombination of D_2^+ is the dominating source of Balmer-α emission(Figs. 6d, e, f). Volume recombination contributes approximately 20% of the peak emission in partially detached conditions ($n_{e,sep,LFS-mp} = 1.8 \cdot 10^{19}$ m^{-3}), compared to 70% contribution of D_2^+. Since the density of the molecular ion D_2^+ is calculated using the rate for hydrogen, the emission is likely overestimated. Due to the higher mass of deuterium, the equivalent collision cross-sections for deuterium should be shifted to higher energies, which would cause the density of the D_2^+ ions to be lower at the same electron temperature as for H_2^+. Additional uncertainty is caused by the approximation $T_{D_2} = 0.1$ eV used in calculating the $D_2 + D^+$ charge-exchange reaction. To have an accurate estimate of the D_2^+ emission, a three parameter rate in n_{D^+}, T_{D^+} and T_{D_2} is needed to resolve $n_{D_2^+}$, thus, the emission. In the simulations, the intensity of the Balmer-α emission stagnates at $n_{e,sep,LFS-mp} = 1.8 \cdot 10^{19}$ m^{-3} (Figs. 6e, f), which implies that too little power reaches the LFS divertor, as the measured Balmer emission is three times higher than predicted.

The EDGE2D-EIRENE predicted Balmer-γ emission is dominated by electron impact excitation in low-recycling conditions (Fig. 7a), as is expected in ionizing plasma conditions. In high-recycling conditions, and at the onset of detachment, a second Balmer-γ peak is formed (Figs. 7b, c, d), which is caused by the dissociative recombination of the D_2^+ molecules. Transitioning from high-recycling to detached conditions, the intensity of the Balmer-γ emission increases by a factor of 5. In the detached conditions, volume recombination of electrons and deuterium ions is the dominant source of Balmer-γ emission (Figs. 7e, f), contributing approximately 70% of the emission. Therefore, the increase in the ratio of Balmer-γ to Balmer-α emission in detached conditions is a signature of volume recombination.

Investigations with a higher input power at 2.8 MW in detached conditions ($n_{e,sep,LFS-mp} = 2.2 \cdot 10^{19}$ m^{-3}) results in improved agreement in the EDGE2D-EIRNE predicted and measured Balmer-α and Balmer-γ emission (Figs. 8a, b, c). For Balmer-α, the predicted emission at the peak is within 40% of the measured emission. For Balmer-γ the simulation and the experiment agrees on the emission inboard of the strike-point. In the far-SOL, a sharp peak in the predicted Balmer-γ is observed. At $n_{e,sep,LFS-mp} = 1.8 \cdot 10^{19}$ m^{-3} (not shown), the peak emission is increased by 15%, i.e. the stagnation point of the emissions moves to higher $n_{e,sep,LFS-mp}$. Additionally, at $n_{e,sep,LFS-mp} = 2.2 \cdot 10^{19}$ m^{-3} the electron density at the LFS target increases by 30% with increased power entering the SOL. Therefore, increasing the power reaching the divertor SOL allows for increasing the plasma density, thus, neutrals, which results in increased emission by a factor of 2. However, there are uncertainties in the D_2^+ contribution to the Balmer line emission, thus, if the D_2^+ density profile is fully resolved, even more power and higher plasma density may be required to reach agreement between simulations and measurements.

Increasing the simulation core input power is a proxy for increasing the power entering the divertor SOL. The input power value of 2.8 MW is likely nonphysical, since the total heating power in detached conditions is 2.7 to 3.0 MW, i.e. at an input power of 2.8 MW the core impurity line-radiation is omitted. In the EDGE2D-EIRENE simulations power is also lost to the main chamber walls, thus, if less power is lost to the main chamber walls, more has to be transported into the divertor SOL, which raises the emission limit. Therefore, if the fall-off length of n_e was shorter in the simulations, more power would be transported over to the divertor SOL. To match experiment requires adjusting the input power, the radial transport of heat and particles, in conjunction with the control density. Increasing the power entering the divertor SOL increases the emission limit, which can be reached by increasing the plasma density, i.e. by increasing the control density $n_{e,sep,LFS-mp}$.

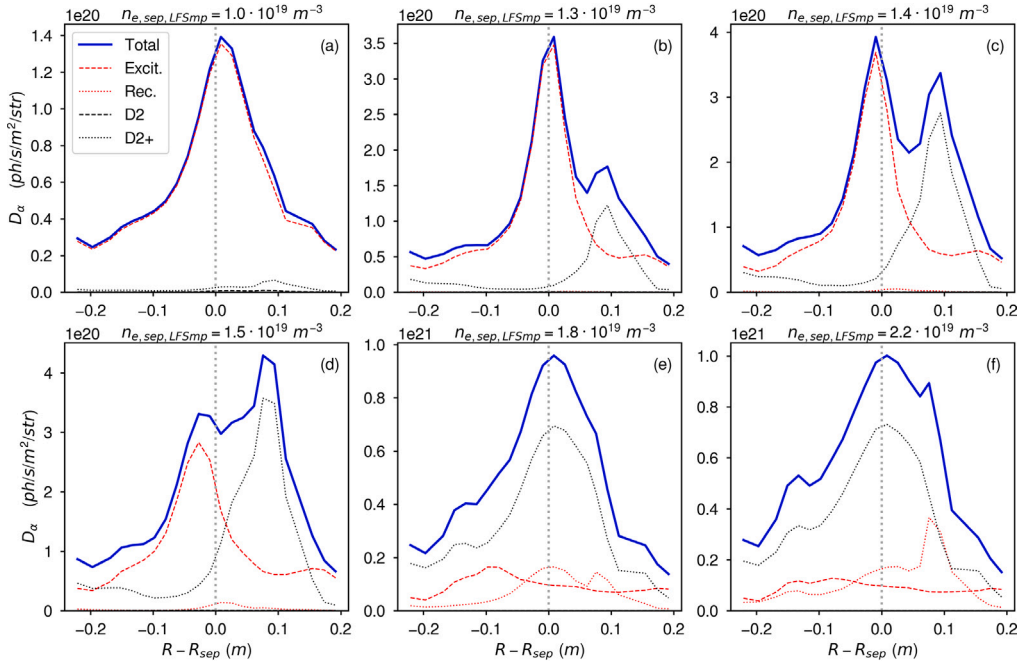

Fig. 6. EDGE2D-EIRENE predicted Balmer-α line emission (blue, solid, sum of the sources) as a function of distance from the separatrix at the target surface, separated into sources due to electron impact excitation (red, dashed), recombination (red, dotted), molecular dissociation (black, dashed), dissociative recombination of molecular ions (black, dotted), and neutralization (green, dot), at the low-field side in low-recycling conditions (a), in high-recycling conditions (b, c, d), in partially detached conditions (e), and in the simulation electron density limit (f). The dashed grey line marks the separatrix position at the target surface. (For interpretation of the references to colour in this figure legend, the reader is referred to the web version of this article.)

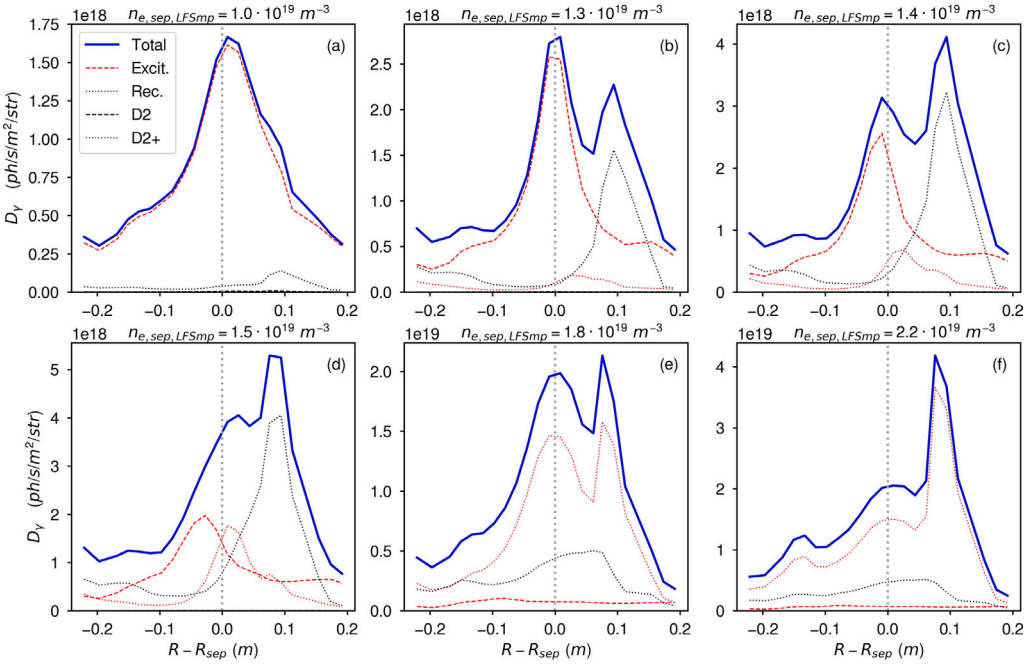

Fig. 7. EDGE2D-EIRENE predicted Balmer-γ line emission (blue, solid, sum of the sources) as a function of distance from the separatrix at the target surface, separated into sources due to electron impact excitation (red, dashed), recombination (red, dotted), molecular dissociation (black, dashed), dissociative recombination of molecular ions (black, dotted), and neutralization (green, dot), at the low-field side in low-recycling conditions (a), in high-recycling conditions (b, c, d), in partially detached conditions (e), and in the simulation electron density limit (f). The dashed grey line marks the separatrix position at the target surface. (For interpretation of the references to colour in this figure legend, the reader is referred to the web version of this article.)

4. Conclusions

The evolution of the EDGE2D-EIRENE predicted Balmer-γ to Balmer-α emission ratio from low-recycling to detached conditions is in qualitative agreement with the measured ratio. In the simulations, volume recombination of electrons and the fuel ions is the primary source of the Balmer-γ line emission in detached conditions, thus, the increase in the ratio signifies the presence of volume recombination. Additionally, the EDGE2D-EIRENE predicted emission stagnates in detached conditions with increasing n_e, similarly to experiment, but a factor of 2.5 lower than measured. The discrepancy is partially solved by increasing the core input power in conjunction with the control

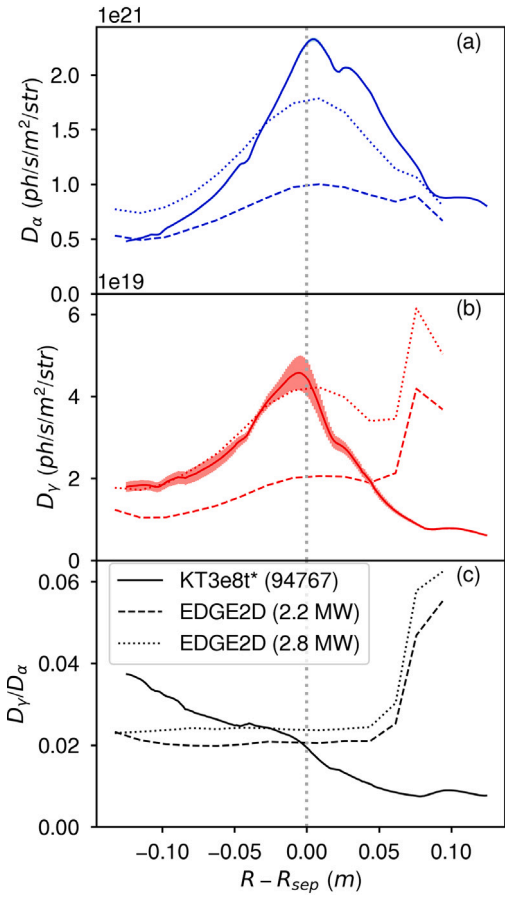

Fig. 8. EDGE2D-EIRENE predicted (2.2 MW, dashed, 2.8 MW, dotted) and KT3e8ta/b measured (solid) Balmer-α (a) and Balmer-γ (b) emission, and the ratio Balmer-γ to Balmer-α (c), on the LFS divertor. The dashed vertical line marks the location of the strike-point.

plasma density. The increase in core input power increases the power entering the divertor SOL, which increases the limit of the emission. When the control density $n_{e,sep,LFS-mp}$ is increased to $2.2 \cdot 10^{19}$ m^{-3} with 2.8 MW of core input power, the predicted emission increases by a factor of 2. However, a discrepancy of a factor of 1.5 between the simulation and experiments remains in the observed emission.

In all plasma conditions, the EDGE2D-EIRENE predicted emission profiles have longer fall-off lengths compared to experiment. Due to the longer fall-off length of the SOL in the simulations, there are more plasma particles in the far-SOL, which is observed as a sharp peak in the Balmer-γ emission. Systematically, EDGE2D-EIRENE underestimates the electron density and overestimates the electron temperature in the near-SOL. In the far-SOL the effect is reversed, i.e. EDGE2D-EIRENE overestimates n_e and underestimates T_e. To match the simulations with experiment, the input power and the radial transport of heat and particles in EDGE2D-EIRENE need to be adjusted, in conjunction with the control plasma density $n_{e,sep,LFS-mp}$. With a shorter SOL fall-off length, less heat is transferred to the main chamber walls, thus, more power is transported into the divertor SOL. Increasing the power density in the EDGE2D-EIRENE simulations would allow for higher electron density and neutral density, thus, higher emission.

The inclusion of other missing physics phenomena, such as the inclusion of photon opacity, to the coupled simulation need to be investigated. In Ref. [23], it is shown that in standalone EIRENE simulations the inclusion of Lyman-opacity increased Balmer-α radiation by 50%, which excludes the impact of reflections. Similarly, in Ref. [24] the derived opacity corrected rates for Balmer-α emission show higher emission by a factor of 5 to 8, when $T_e > 1.0$ eV, compared to rates which assume that the plasma is optically thin. A fundamental limitation of the *ad-hoc* diffusive model in EDGE2D-EIRENE remains, which is that the radial transport of heat and particles in the SOL is turbulent in reality, not diffusive. In Ref. [25], a convection-dominated model was applied to SOLPS, and it was found that in detached conditions the predicted high-field side target density reproduces the measured density, while the diffusive model does not. However, the electron temperature was still underpredicted by a factor of 4 to 6, which shows the limitation of the *ad-hoc* convective model.

At the onset of detachment, in the EDGE2D-EIRENE simulations, a D_2^+ front forms in the far-SOL, which moves towards the strike-point with increasing degree of detachment. The double peak structure predicted by EDGE2D-EIRENE, which is caused by the D_2^+ front, is observed in the experiment in high-recycling conditions. Simulations with a simplified grid show that the secondary peak is due to the step in the tile-5 to tile-6 transition, since a secondary peak is not observed in the simplified grid. The plasma temperature decreases proportionally to the tile-5 to tile-6 gap, which is causes a proportionally higher neutral densities in the region, causing higher observed emission. Therefore, including accurate geometric description of the divertor in the simulations is important to properly capture the emission profiles.

In the simulations, the dissociative recombination of the D_2^+ ions becomes the dominant source of the Balmer-γ line emission in detached conditions, but there are uncertainties in the calculation of the D_2^+ density. The molecular ion density $n_{D_2^+}$, which is used in calculating the line emission, is calculated using the AMJUEL rate for hydrogen, which is not fully valid in regions of plasma with low deuterium ion temperature, since the charge-exchange process $H_2 + H^+ \rightarrow H_2^+ + H$ depends on the isotope mass, and is different for deuterium. To accurately assess the impact of the molecular ions D_2^+ on the Balmer emission, three parameter cross-sections of the charge-exchange process $D_2 + D^+ \rightarrow D_2^+ + D$, the primary source of D_2^+, in n_{D^+}, T_{D^+}, and T_{D_2} is required.

The ratios of Balmer-lines characterize the recycling conditions with great accuracy. Qualitatively, EDGE2D-EIRENE reproduces the evolution of the average Balmer-γ/Balmer-α ratio. The EDGE2D-EIRENE simulations are compared to experiment with varied conditions, including different recycling conditions, different simulation input power, and with simple and complex divertor geometries, which allows for inferring the sources of emission in experiment accurately. Therefore, from a divertor-design point-of-view, the visible light hydrogenic Balmer-line diagnostics offers easy access to monitoring the divertor conditions, which is crucial in operating the divertor. Based on the EDGE2D-EIRENE predictions, the Balmer-γ line can be utilized in detecting regions, in which volume recombination of plasma occurs, since the Balmer-γ emission is dominated by recombination.

CRediT authorship contribution statement

Vesa-Pekka Rikala: Writing – review & editing, Writing – original draft, Visualization, Validation, Methodology, Formal analysis, Conceptualization. **M. Groth:** Writing – review & editing, Supervision, Project administration, Methodology, Investigation, Conceptualization. **A.G. Meigs:** Software, Investigation, Formal analysis, Data curation. **D. Reiter:** Formal analysis. **B. Lomanowski:** Investigation, Data curation. **S. Aleiferis:** Investigation, Data curation. **G. Corrigan:** Investigation, Data curation. **I.S. Carvalho:** Investigation, Data curation. **D. Harting:** Investigation, Conceptualization. **N. Horsten:** Investigation, Formal analysis, Data curation. **I. Jepu:** Investigation, Data curation. **J. Karhunen:** Investigation, Data curation. **K.D. Lawson:** Investigation, Data curation. **C. Lowry:** Investigation, Data curation. **S. Menmuir:** Investigation, Data curation. **B. Thomas:** Investigation, Data curation. **D. Borodin:** Investigation, Data curation. **D. Douai:** Investigation, Data curation. **A. Huber:** Investigation, Data curation.

Declaration of competing interest

The authors declare the following financial interests/personal relationships which may be considered as potential competing interests: Vesa-Pekka Rikala reports financial support was provided by European Consortium for the Development of Fusion Energy. If there are other authors, they declare that they have no known competing financial interests or personal relationships that could have appeared to influence the work reported in this paper.

Acknowledgements

This work has been carried out within the framework of the EUROfusion Consortium, funded by the European Union via the Euratom Research and Training Programme (Grant Agreement No 101052200 — EUROfusion). Views and opinions expressed are however those of the author(s) only and do not necessarily reflect those of the European Union or the European Commission. Neither the European Union nor the European Commission can be held responsible for them.

Appendix A. Data

EDGE2D-EIRENE version v210921 was used, and the catalogue names for the cases are, in increasing control $\langle n_e \rangle$ order:

mgroth/81472/aug0122/seq#1
mgroth/81472/aug0222/seq#1
mgroth/81472/jul3122/seq#1
mgroth/81472/aug0522/seq#2
mgroth/81472/aug0522/seq#3
mgroth/81472/aug0322/seq#3.

For $P_{core} = 2.8$ MW, the catalogue names are:

mgroth/81472/apr1724/seq#1
mgroth/81472/apr0724/seq#1.

The catalogue name for the raised tile-6 case is:
mgroth/80295/apr0518/seq#2.

Appendix B. AMJUEL rates used in calculating the atomic and molecular contribution to deuterium line emission

H.12 2.1.5a	Balmer-α	H excitation
H.12 2.1.5d	Balmer-γ	H excitation
H.12 2.1.8a	Balmer-α	H recombination
H.12 2.1.8d	Balmer-γ	H recombination
H.12 2.2.5a	Balmer-α	H_2 dissociation
H.12 2.2.5d	Balmer-γ	H_2 dissociation
H.12 2.2.14a	Balmer-α	H_2^+ dissociation
H.12 2.2.14d	Balmer-γ	H_2^+ dissociation
H.12 2.0c	$n_{H_2^+}/n_{H_2}$	Ratio of densities

Data availability

Data will be made available on request.

References

[1] A.W. Leonard, Plasma detachment in divertor tokamaks, Plasma Phys. Control. Fusion 60 (4) (2018) 044001, http://dx.doi.org/10.1088/1361-6587/aaa7a9.
[2] G.M. McCracken, M.F. Stamp, R.D. Monk, A.G. Meigs, J. Lingertat, R. Prentice, A. Starling, R.J. Smith, A. Tabasso, Evidence for volume recombination in JET detached divertor plasmas, Nucl. Fusion 38 (4) (1998) 619, http://dx.doi.org/10.1088/0029-5515/38/4/311.
[3] R.C. Isler, G.R. McKee, N.H. Brooks, W.P. West, M.E. Fenstermacher, R.D. Wood, Signatures of deuterium recombination in the DIII-D divertor, Phys. Plasmas 4 (8) (1997) 2989–2996, http://dx.doi.org/10.1063/1.872432.
[4] A. Huber, S. Wiesen, M. Bernert, S. Brezinsek, A.V. Chankin, G. Sergienko, V. Huber, P. Abreu, A. Boboc, M. Brix, D. Carralero, E. Delabie, T. Eich, H.G. Esser, C. Guillemaut, S. Jachmich, E. Joffrin, A. Kallenbach, U. Kruezi, P. Lang, Ch. Linsmeier, C.G. Lowry, C.F. Maggi, G.F. Matthews, A.G. Meigs, Ph. Mertens, F. Reimold, J. Schweinzer, G. Sips, M. Stamp, E. Viezzer, M. Wischmeier, H. Zohm, JET contributors, ASDEX Upgrade Team, The effect of the isotope on the H-mode density limit, Nucl. Fusion 57 (8) (2017) 086007, http://dx.doi.org/10.1088/1741-4326/aa663a.
[5] J. Karhunen, M. Carr, J.R. Harrison, B. Lomanowski, I. Balboa, P. Carvalho, M. Groth, A. Huber, G.F. Matthews, A. Meakins, S. Silburn, JET Contributors, Effect of reflections on 2D tomographic reconstructions of filtered cameras and on interpreting spectroscopic measurements in the JET ITER-like wall divertor, Rev. Sci. Instrum. 90 (10) (2019) 103504, http://dx.doi.org/10.1063/1.5118885.
[6] A Taroni, G Corrigan, G Radford, R Simonini, J Spence, S Weber, The multi-fluid codes EDGE1D and EDGE2D: Models and results, Contrib. Plasma Phys. 32 (3–4) (1992) 438–443, http://dx.doi.org/10.1002/ctpp.2150320339.
[7] D. Reiter, M. Baelmans, P. Börner, The EIRENE and B2-EIRENE codes, Fusion Sci. Technol. 47 (2) (2005) 172–186, http://dx.doi.org/10.13182/FST47-172.
[8] S. Wiesen, D. Reiter, V. Kotov, M. Baelmans, W. Dekeyser, A.S. Kukushkin, S.W. Lisgo, R.A. Pitts, V. Rozhansky, G. Saibene, I. Veselova, S. Voskoboynikov, The new SOLPS-ITER code package, J. Nucl. Mater. 463 (2015) 480–484, http://dx.doi.org/10.1016/j.jnucmat.2014.10.012, PLASMA-SURFACE INTERACTIONS 21.
[9] M. Carr, A. Meakins, A. Baciero, M. Bernert, A. Callarelli, A. Field, C. Giroud, J. Harrison, N. Hawkes, S. Henderson, B. Lipschultz, Towards integrated data analysis of divertor diagnostics with ray-tracing, EPS Conf. Plasma Phys. 44 (2017).
[10] K Verhaegh, B Lipschultz, C Bowman, B P Duval, U Fantz, A Fil, J R Harrison, D Moulton, O Myatra, D Wünderlich, F Federici, D S Gahle, A Perek, M Wensing, the TCV Team, the EuroFusion MST1 Team, A novel hydrogenic spectroscopic technique for inferring the role of plasma–molecule interaction on power and particle balance during detached conditions, Plasma Phys. Control. Fusion 63 (3) (2021) 035018, http://dx.doi.org/10.1088/1361-6587/abd4c0.
[11] J Karhunen, A Holm, B Lomanowski, V Solokha, S Aleiferis, P Carvalho, M Groth, K D Lawson, A G Meigs, A Shaw, JET Contributors, Experimental distinction of the molecularly induced balmer emission contribution and its application for inferring molecular divertor density with 2D filtered camera measurements during detachment in JET L-mode plasmas, Plasma Phys. Control. Fusion 64 (7) (2022) 075001, http://dx.doi.org/10.1088/1361-6587/ac6ae3.
[12] D. Reiter, The data file AMJUEL: Additional Atomic and Molecular Data for EIRENE, Technical report, FZ Juelich, 2000.
[13] A. Boboc, M. Gelfusa, A. Murari, P. Gaudio, JET-EFDA Contributors, Recent developments of the JET far-infrared interferometer-polarimeter diagnostic, Rev. Sci. Instrum. 81 (10) (2010) 10D538, http://dx.doi.org/10.1063/1.3478146.
[14] M. Groth, S. Brezinsek, P. Belo, M.N.A. Beurskens, M. Brix, M. Clever, J.W. Coenen, C. Corrigan, T. Eich, J. Flanagan, C. Guillemaut, C. Giroud, D. Harting, A. Huber, S. Jachmich, U. Kruezi, K.D. Lawson, M. Lehnen, C. Lowry, C.F. Maggi, S. Marsen, A.G. Meigs, R.A. Pitts, G. Sergienko, B. Sieglin, C. Silva, A. Sirinelli, M.F. Stamp, G.J. van Rooij, S. Wiesen, the JET-EFDA Contributors, Impact of carbon and tungsten as divertor materials on the scrape-off layer conditions in JET, Nucl. Fusion 53 (9) (2013) 093016.
[15] K.D. Lawson, R. Barnsley, C.F. Maggi, S. Tyrrell, M. Beldishevski, J. Brzozowski, M. Buckley, G. Cass, T. Elevant, S. Griph, P. Heesterman, C. Hogben, M. Jennison, M.F. Stamp, J. Williams, K.-D. Zastrow, JET-EFDA Contributors, Enhancements to the JET poloidally scanning vacuum ultraviolet/visible spectrometers, Rev. Sci. Instruments 83 (10) (2012) 10D536, http://dx.doi.org/10.1063/1.4745213.
[16] P.D. Morgan, K.H. Behringer, P.G. Carolan, M.J. Forrest, N.J. Peacock, M.F. Stamp, Spectroscopic measurements on the Joint European Torus using optical fibers to relay visible radiation, Rev. Sci. Instruments 56 (5) (1985) 862–864, http://dx.doi.org/10.1063/1.1138074.
[17] A.G. Meigs, S. Brezinsek, M. Clever, A. Huber, S. Marsen, C. Nicholas, M. Stamp, K.-D. Zastrow, Deuterium Balmer/Stark spectroscopy and impurity profiles: First results from mirror-link divertor spectroscopy system on the JET ITER-like wall, J. Nucl. Mater. 438 (2013) S607–S611, http://dx.doi.org/10.1016/j.jnucmat.2013.01.127.
[18] B.A. Lomanowski, A.G. Meigs, N.J. Conway, K.-D. Zastrow, R.M. Sharples, P. Heesterman, D. Kinna, JET EFDA Contributors, Enhanced visible and near-infrared capabilities of the JET mirror-linked divertor spectroscopy system, Rev. Sci. Instrum. 85 (11) (2014) 11E432, http://dx.doi.org/10.1063/1.4893426.

[19] A. Huber, S. Brezinsek, Ph. Mertens, B. Schweer, G. Sergienko, A. Terra, G. Arnoux, N. Balshaw, M. Clever, T. Edlingdon, S. Egner, J. Farthing, M. Hartl, L. Horton, D. Kampf, J. Klammer, H.T. Lambertz, G.F. Matthews, C. Morlock, A. Murari, M. Reindl, V. Riccardo, U. Samm, S. Sanders, M. Stamp, J. Williams, K.D. Zastrow, C. Zauner, A new radiation-hard endoscope for divertor spectroscopy on JET, Fusion Eng. Des. 88 (6) (2013) 1361–1365, http://dx.doi.org/10.1016/j.fusengdes.2013.02.053, Proceedings of the 27th Symposium On Fusion Technology (SOFT-27); Liège, Belgium, September 24-28, 2012.

[20] H P Summers, W J Dickson, M G O'Mullane, N R Badnell, A D Whiteford, D H Brooks, J Lang, S D Loch, D C Griffin, Ionization state, excited populations and emission of impurities in dynamic finite density plasmas: I. The generalized collisional–radiative model for light elements, Plasma Phys. Control. Fusion 48 (2) (2006) 263, http://dx.doi.org/10.1088/0741-3335/48/2/007.

[21] D. Reiter, The data file HYDHEL: Atomic and Molecular Data for EIRENE, Technical report, FZ Juelich, 2002.

[22] B. Lomanowski, M. Carr, A. Field, M. Groth, A.E. Jaervinen, C. Lowry, A.G. Meigs, S. Menmuir, M. O'Mullane, M.L. Reinke, C.K. Stavrou, S. Wiesen, Spectroscopic investigation of N and Ne seeded induced detachment in JET ITER-like wall L-modes combining experiment and EDGE2D modeling, Nucl. Mater. Energy 20 (2019) 100676, http://dx.doi.org/10.1016/j.nme.2019.100676.

[23] Ray Chandra, Detlev Reiter, Niels Horsten, Mathias Groth, Lyman line opacities in tokamak divertor plasmas under high-recycling and detached conditions, Nucl. Mater. Energy 41 (2024) 101794, http://dx.doi.org/10.1016/j.nme.2024.101794.

[24] J. Karhunen, B. Lomanowski, S. Aleiferis, P. Carvalho, M. Groth, A. Holm, K.D. Lawson, A.G. Meigs, A. Shaw, V. Solokha, Addressing the impact of Lyman opacity in inference of divertor plasma conditions with 2D spectroscopic camera analysis of Balmer emission during detachment in JET L-mode plasmas, Submitt. Nucl. Mater. Energy 42 (2025) 101880, http://dx.doi.org/10.1016/j.nme.2025.101880, https://www.sciencedirect.com/science/article/pii/S2352179125000201.

[25] J. Karhunen, M. Groth, D.P. Coster, D. Carralero, L. Guimarais, V. Nikolaeva, S. Potzel, T. Pütterich, F. Reimold, A. Scarabosio, E. Viezzer, M. Wischmeier, SOLPS 5.0 simulations of the high-field side divertor detachment of L-mode plasmas in ASDEX upgrade with convection-dominated radial SOL transport, Nucl. Mater. Energy 19 (2019) 279–286, http://dx.doi.org/10.1016/j.nme.2019.02.040.